BULLETIN
OF "CAROL I" NATIONAL DEFENCE UNIVERSITY

https://buletinul.unap.ro/index.php/en/

Detection of Buried Landmines using a Convolutional Autoencoder trained on Simulated prompt Gamma Spectra

Konstantinos KARAFASOULIS, PhD*

*Laboratory Teaching Staff, Hellenic Army Academy, Athens, Greece
e-mail: ckaraf@gmail.com

Abstract

The detection of buried landmines remains a persistent challenge in security and humanitarian demining. In this work, we present an indirect detection methodology based on the analysis of prompt gamma-ray emissions induced by 14 MeV neutron irradiation. A high-resolution $LaBr_3$ detector captures the gamma spectra arising from neutron interactions with soil constituents and buried explosives. A Convolutional Neural Network (CNN) autoencoder, trained in an unsupervised manner, models the intrinsic spectral response of soil under varying moisture conditions. Anomalies between reconstructed and measured spectra are used to infer the presence of subsurface anomalies consistent with landmines. Monte Carlo simulations, conducted with the Geant4 toolkit, generate a comprehensive dataset encompassing a soil matrix under various moisture levels. The proposed system demonstrates sensitivity to buried antipersonnel landmines at shallow depths, validating the integration of neutron activation analysis and deep learning for advanced landmine detection applications.

Keywords:
Landmine Detection; Artificial Intelligence; Autoencoders; Anomaly Detection; Neutron Activation; Gamma Radiation.

Article info
Received: 12 May 2025; Revised: 6 June 2025; Accepted: 10 June 2025; Available online: 27 June 2025

Citation: Karafasoulis, K. 2025. "Detection of Buried Landmines using a Convolutional Autoencoder trained on Simulated prompt Gamma Spectra." *Bulletin of "Carol I" National Defence University*, 14(2): 114-127. https://doi.org/10.53477/2284-9378-25-19

© „Carol I" National Defence University Publishing House
This article is an open access article distribted under the terms and conditions of the Creative Commons Attribution (CC BY-NC-SA)

The global impact of landmines, particularly anti-personnel and anti-tank devices, continues to be a significant humanitarian and security concern. According to (Landmine and Cluster Munition Monitor 2024), at least 58 countries remain affected by these hidden threats, which cause thousands of casualties annually, the majority of whom are civilians. Beyond the tragic human cost, landmines pose long-term socio-economic barriers by rendering agricultural lands unusable, displacing populations, and impeding post-conflict recovery. From a military standpoint, effective detection and clearance of landmines are also of strategic importance, as they directly affect troop mobility, operational planning, and the safety of personnel in both combat and peacekeeping missions. Consequently, advancing landmine detection technologies serves both humanitarian objectives and tactical military needs, reinforcing global stability and mission success in affected regions.

Conventional landmine detection technologies include metal detectors, ground-penetrating radar (GPR), and trained detection animals (e.g., dogs or rats). While these methods have proven utility, each comes with critical limitations. Metal detectors suffer from high false-positive rates due to metallic clutter in post-conflict zones, while GPR performance can be significantly degraded by soil heterogeneity or high moisture content. Biological detection methods, although accurate, are resource-intensive and difficult to deploy at scale.

To overcome these limitations, nuclear-based techniques, particularly those exploiting neutron interrogation, offer unique advantages. One such technique is Prompt Gamma Neutron Activation Analysis (PGNAA), which relies on bombarding the ground with fast neutrons (e.g., 14 MeV) and detecting the resulting prompt gamma rays emitted when the neutrons interact with various nuclei in the soil and hidden objects. PGNAA enables non-destructive elemental analysis, particularly effective in detecting nitrogen, a key component of many explosive compounds such as TNT, RDX, and PETN.

Gamma-ray lines commonly associated with explosive materials include:

- 10.8 MeV (from the reaction $^{14}N(n,\gamma)^{15}N$)
- 2.22 MeV (from $^{1}H(n,\gamma)^{2}H$)
- 6.13 MeV (from $^{16}O(n,n'\gamma)^{16}O$)

The presence of these characteristic gamma lines can indicate anomalies beneath the surface. However, interpreting this spectral information is not trivial. Gamma spectra are influenced by numerous environmental variables, including soil composition, moisture content, density, and the presence of innocuous materials (e.g., plastic waste, buried vegetation). These confounding factors can lead to false positives when using rule-based or threshold-based detection approaches.

To address this complexity, we propose a machine learning-based solution utilising a Convolutional Neural Network (CNN) autoencoder. A CNN autoencoder is a type of neural network trained to compress and reconstruct its input—in this case, the full gamma spectrum recorded by a $LaBr_3$ detector. During training, the autoencoder learns to represent the "normal" variability of gamma spectra from soil-only conditions, without requiring examples containing landmines. This unsupervised learning paradigm provides several strategic benefits:

- **No need for explosive training data:** Since acquiring real spectra from buried landmines is dangerous, scarce, and often ethically restricted, training exclusively on simulated or measured background soil spectra removes this dependency.
- **Anomaly detection capability:** Once trained, the autoencoder can identify deviations from the learned spectral patterns. When a spectrum from soil containing a buried landmine is input, it cannot be reconstructed accurately, resulting in a high reconstruction error, which flags it as anomalous.
- **Low false positive sensitivity:** Because the model captures the complex spectral variability of legitimate background conditions, it is less prone to overreacting to harmless but structurally different materials that might affect threshold-based systems.

In this paper, we present a simulation-driven study using Geant4 to generate prompt gamma spectra for one soil type at varying moisture levels (0%, 10%, and 20%). A CNN autoencoder is trained solely on these background spectra and evaluated against test cases containing an anti-personnel landmine buried at 5 cm and 10 cm depths. The spectra span 2048 bins up to 15 MeV, reflecting high-resolution detection capabilities. This approach enables robust anomaly detection, even in diverse and noisy soil environments, with high potential for real-world deployment in both humanitarian demining and military applications.

Related Work

Landmine detection has long been a multidisciplinary challenge, combining geophysics, nuclear physics, and increasingly, artificial intelligence. Classical methods such as metal detectors, ground-penetrating radar (GPR), and infrared imaging are widely used but struggle with specific limitations: metal detectors generate high false-positive rates in cluttered environments, GPR sensitivity drops in heterogeneous or moist soil, and infrared sensors are easily confounded by surface conditions.

As a result, neutron-based techniques have emerged as highly promising alternatives due to their ability to probe elemental composition rather than just physical or metallic properties. Among these, Prompt Gamma Neutron Activation Analysis (PGNAA) and Neutron Backscattering (NBT) have received considerable attention. PGNAA, in particular, utilises fast neutrons (e.g., 14 MeV) to induce prompt gamma-ray emissions that reveal elemental signatures, such as those from nitrogen, a common marker for high explosives.

Experimental and simulation studies have validated the effectiveness of nuclear-based systems for detecting explosives. For example, (Elsheikh 2018) modelled a thermal neutron-induced gamma-ray sensor to detect prompt gamma emissions from $^{14}N(n,\gamma)^{15}N$ reactions, capturing the key 10.8 MeV gamma line. Similarly, (Viesti, et al. 2006) demonstrated the use of neutron backscattering techniques for humanitarian demining, emphasising the importance of minimising soil moisture to enhance detection contrast. Additional experimental validation was carried out by specialists (Clifford, et al. 2007) who fielded a thermal neutron activation system for military confirmation of buried anti-tank mines, confirming effectiveness up to 30 cm depths under various environmental conditions.

However, nuclear techniques come with their own challenges, particularly interpreting the complex gamma-ray spectra produced during interrogation. Spectra are affected not only by the elemental composition of the explosive but also by the surrounding soil type, density, and humidity. These environmental confounders can induce misleading spectral features and elevate false alarm rates when traditional thresholding or peak-matching methods are used.

To overcome these limitations, machine learning approaches have been introduced (Xue, et al. 2022). They compared multiple supervised learning models, including fully connected neural networks (FCNN), LightGBM, and radial basis function networks (RBF), to classify PGNAA spectra from different explosive burial conditions. They reported over 96% classification accuracy even under high soil moisture conditions using full-spectrum inputs, underscoring the potential of data-driven models over hand-engineered feature extraction.

Yet, supervised methods inherently depend on labelled training data, often requiring spectra containing real landmines or explosive materials—data that is difficult to obtain due to ethical, safety, and logistical constraints. To mitigate this, unsupervised models, particularly autoencoders, offer a robust alternative. Autoencoders are neural networks that learn to reproduce their input data; deviations between input and output (reconstruction error) can be used to detect anomalies. When trained solely on background spectra (e.g., soil without explosives), any significant deviation caused by the presence of a landmine will manifest as a high reconstruction error.

Other studies, such as those by (Datema, et al. 2003) proposed novel imaging approaches using neutron backscattering and Monte Carlo simulations with GEANT4 to localise hydrogen anomalies in the topsoil. These approaches laid the groundwork for simulation-driven training data, critical for training unsupervised models in the absence of real explosive data.

In this paper, we propose a novel landmine detection framework that combines PGNAA spectral interrogation with a convolutional autoencoder trained solely on simulated background spectra. By learning the underlying structure of gamma-ray spectra from soil without explosives, the model detects anomalies based on reconstruction error when exposed to spectra influenced by buried explosives. This unsupervised approach addresses the dual challenges of limited access to real explosive data and complex spectral variability caused by environmental factors. Leveraging convolutional layers, the autoencoder effectively captures localised spectral features, such as gamma peaks and Compton edges, enabling robust detection of nitrogen-rich explosives while maintaining adaptability across diverse field conditions.

Methodology

1.1. Experimental Setup for PGNAA Simulation

The simulation environment for this study replicates a realistic PGNAA (Prompt Gamma Neutron Activation Analysis) system using a 14 MeV fast neutron source placed within a protective and moderating assembly designed to optimise gamma-ray yield while reducing background noise.

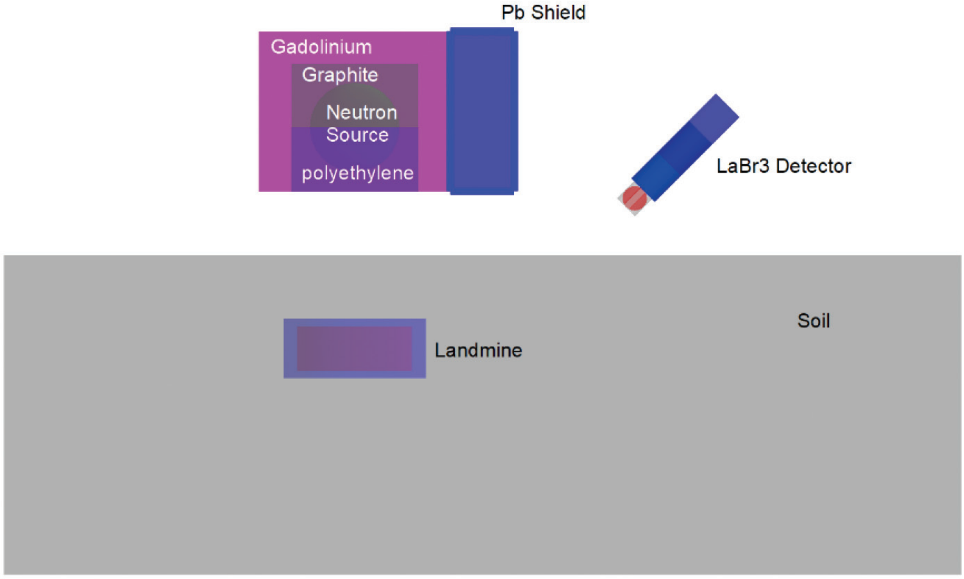

Figure 1 Schematic of the simulation geometry. The neutron source is located at the centre of a hollow spherical shell enclosed in a gadolinium-lined box (open at the bottom). The upper hemisphere of the shell is graphite for neutron reflection, while the lower hemisphere is polyethylene for neutron moderation. The assembly is suspended 10 cm above the soil surface. A lead shield is positioned between the source and the $LaBr_3$ detector to suppress unwanted gamma flux. Simulations include buried mines at 5 cm or 10 cm depth within a 150 cm × 160 cm × 50 cm soil volume.

The neutron source is placed at the centre of a hollow spherical shell with a radius of 7 cm, housed within a gadolinium-lined box measuring 30 cm × 30 cm × 25 cm, open at the bottom. The spherical shell surrounding the source is divided into two hemispheres: the upper half is composed of graphite, serving as a neutron reflector to direct neutrons downward toward the soil, while the lower half is made of polyethylene, acting as a moderator to thermalise fast neutrons.

This configuration enhances the likelihood of neutron interactions within the target medium. The entire assembly is positioned 10 cm above the ground surface. For simulations involving buried mines, the mine is located at a depth of 5 cm or 10 cm within a soil volume measuring 150 cm × 160 cm × 50 cm (depth). The detailed geometry of the mine is presented in Table 3. In control simulations without the mine, the same soil setup is used to evaluate the background response.

A lead (Pb) shield is placed to the right of the source, between the source and the $LaBr_3$ detector, to attenuate scattered and prompt gamma rays from unwanted directions. This shielding improves signal clarity and reduces detector saturation. The detector is located 50 cm away from the source at an inclination angle of 45°, providing an optimised detection geometry for capturing prompt gamma emissions resulting from neutron interactions in the soil.

1.2. Gamma Spectrum Dataset Generation

All gamma-ray spectra used in this study were generated using the Geant4 Monte Carlo simulation toolkit (Agostinelli, et al. 2003). The target region in the simulation consists of one soil type, simulated under three distinct moisture conditions: 0%, 10%, and 20% by weight. Soil compositions, elemental content, and density parameters are detailed in Table 1.

TABLE NO. 1
Soil Composition

Humidity	0%	10%	20%
Density (g/cm^3)	1.47	1.63	1.84
Elements	**Mass Fraction**		
Na	0.008	0.007	0.007
H	0.000	0.011	0.022
K	0.022	0.019	0.017
Mg	0.032	0.029	0.026
Ca	0.037	0.034	0.051
Fe	0.064	0.058	0.030
Al	0.071	0.064	0.057
Si	0.296	0.267	0.237
O	0.470	0.511	0.553

To ensure a statistically robust gamma emission profile, a total of 750,000 gamma-ray interaction events in the detector were recorded, resulting from neutron interactions with soil at three different moisture levels: dry, 10%, and 20% moisture. Specifically, 250,000 gamma-ray events were collected for each soil condition following neutron-induced reactions. The deposited energy spectra on the $LaBr_3$ detector were then processed to reflect the detector's intrinsic energy resolution by applying Gaussian smearing to the recorded gamma energies, using a full width at half maximum (FWHM) defined as:

$$FWHM = A\sqrt{\frac{E}{E_c}} \tag{1}$$

where A = 19.2 keV and E_c = 662 keV. This smearing procedure accurately reflects the energy resolution characteristics of the $LaBr_3$ detector, thereby enhancing the realism of the simulated spectra.

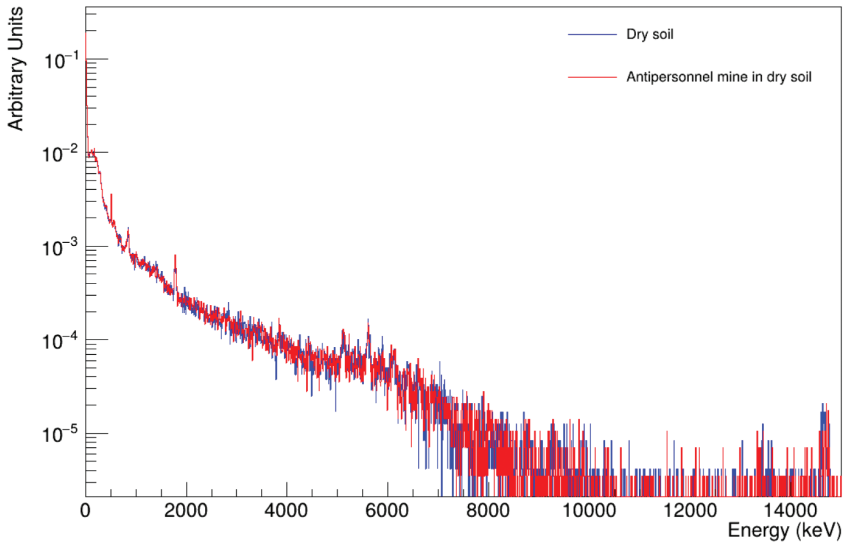

Figure 2 Comparison of gamma-ray spectra following neutron activation. The blue line represents the spectrum of dry soil alone, while the orange line corresponds to dry soil containing a buried antipersonnel landmine at a depth of 5 cm. The presence of the landmine induces characteristic spectral features, distinguishing it from the background soil response.

Subsequently, 10,000 gamma spectra were generated per soil composition from the smeared interaction dataset. Each spectrum was constructed by randomly sampling the simulated events, promoting statistical diversity and improving dataset robustness. These spectra consisted of 2,048 discrete energy bins, spanning the full dynamic range of the $LaBr_3$ detector (0–15 MeV), with each spectrum normalised to a total of 50,000 events. Representative gamma spectra for dry soil and the landmine model buried in dry soil at 5cm depth are presented in Figure 2.

1.3. CNN Autoencoder Architecture

To model the background spectral distribution and perform anomaly detection, a 1D Convolutional Neural Network (CNN) autoencoder (Adari and Alla 2024) was implemented using Keras (Gulli and Pal 2017). The architecture was designed to progressively compress high-dimensional spectral data and reconstruct it from a learned latent representation, allowing for anomaly detection via reconstruction error.

TABLE NO. 2
CNN Autoencoder Architecture

Layer Type	Filters	Nodes	Kernel Size	Stride	Activation	Padding
1D Input	-	2048	-	-	-	-
Encoder						
Conv1D	32	-	3	1	ReLU	Same
Max Pooling 1D	-	-	2	2	-	Same
Conv1D	64	-	3	1	ReLU	Same
Max Pooling 1D	-	-	2	2	-	Same
Conv1D	128	-	3	1	ReLU	Same
Max Pooling 1D	-	-	2	2	-	Same
Decoder						
Upsampling 1D	-	-	-	2	-	-
Conv1D	128	-	3	1	ReLU	Same
Upsampling 1D	-	-	-	2	-	-
Conv1D	64	-	3	1	ReLU	Same
Upsampling 1D	-	-	-	2	-	-
Conv1D	32	-	3	1	ReLU	Same
Conv1D	1	-	3	1	Sigmoid	Same
1D Output	-	2048	-	-	-	-

The encoder consists of three convolutional layers with filter sizes of 32, 64, and 128, each using a kernel size of 3, a stride of 1, and 'same' padding. Each convolutional layer is followed by a MaxPooling layer with a pool size of 2 and a stride of 2, which progressively reduces the spatial resolution of the input spectrum while increasing feature depth.

The decoder mirrors the encoder's structure in reverse. It begins with the most compressed latent feature map and reconstructs the full-resolution spectrum using three convolutional layers in reverse order (128 → 64 → 32 filters), interleaved with Upsampling layers to restore the original dimensionality. The final output layer uses a Sigmoid activation function to reproduce the 2048-bin normalised spectrum.
The complete architecture, including kernel parameters and feature map dimensions at each stage, is presented in Table 2.

1.4. Training Procedure

The CNN autoencoder was implemented and trained using the Adam optimiser (Kingma and Ba 2015) with default parameters and a Mean Squared Error (MSE) loss function:

$$\mathrm{MSE} = \frac{1}{2048} \sum_{i=1}^{2048} (y_i - \hat{y}_i)^2 \quad (2)$$

where y_i is the true count in bin i of the real spectrum and $\hat{y}_i$ is the predicted count in bin i by the autoencoder.

The model was trained for 5 epochs using a batch size of 128 spectra. The training dataset, as described in Section 1.2, comprises spectra obtained from three different soil types: dry, 10% moisture, and 20% moisture. To ensure robust model evaluation, 70% of this dataset was used for training and the remaining 30% for validation. The training and validation MSE per batch iteration is shown in Figure 3, which confirms the absence of overfitting. The training curve exhibits a smooth convergence, and the validation loss closely tracks the training loss throughout the epochs.

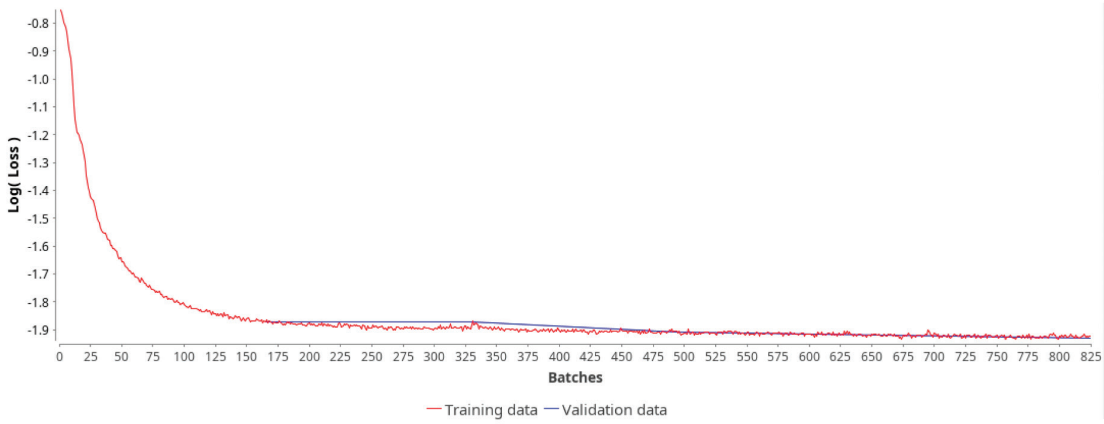

Figure 3 Logarithm of the mean squared error (MSE) per batch during training of the CNN autoencoder. The red curve represents the training samples, while the blue curve corresponds to the validation samples. The close agreement between the two curves indicates stable learning, with no signs of overtraining observed.

Since the model was only trained on spectra representing clean soil, the learned representation reflects the natural variability of soil-only gamma emissions, allowing the system to detect anomalies (i.e., landmine presence) during evaluation.

Model Evaluation

To assess the performance of the CNN autoencoder in detecting buried landmines, we conducted a dedicated set of simulations involving a realistically modelled anti-personnel landmine filled with TNT (trinitrotoluene) (Table no. 3). The simulated explosive object was buried in the dry soil used during training, under identical physical and radiological conditions, thereby ensuring consistent experimental parameters between training and evaluation.

The geometry and chemical composition of the landmine were modelled based on standard anti-personnel ordnance specifications. The explosive material, TNT, was represented using its molecular composition ($C_7H_5N_3O_6$), emphasising the high nitrogen content, which serves as a key elemental indicator in PGNAA-based detection methods. The mine casing was assumed to be made of plastic, consistent with real-world low-metal mines.

TABLE NO. 3
CNN Antipersonnel Mine Specifications

Material	$C_7H_5N_3O_6$),
Mass (kg)	2.939
Density (g/cm^3)	1.65
Shape	Cylindrical
Radius (cm)	7.0
Height (cm)	7.0
Case Material	Low-Density Plastic
Case Width (cm)	2.1

Two burial depths were examined to reflect practical detection thresholds in both humanitarian and military demining operations.

- 5 cm below the soil surface (shallow burial)
- 10 cm below the soil surface (moderate depth)

Using the same PGNAA system configuration described previously — including the graphite reflector, polyethylene moderator, gadolinium box, and lead shielding — we simulated neutron interactions with soil containing the buried landmine.
For each burial depth (5 cm and 10 cm), a total of 300,000 gamma-ray interaction events in the detector were recorded, resulting from neutron interactions with the buried landmine simulated using Geant4. From these events, 10,000 gamma-ray spectra were randomly sampled per depth, with each spectrum consisting of 2,048 energy bins spanning up to 15 MeV. This procedure mirrors the methodology employed for generating the background soil spectra and ensures consistent statistical representation across all evaluation conditions.

Each of the 10,000 landmine-influenced gamma spectra was processed through the trained CNN autoencoder, which had been trained solely on soil-only gamma spectra. To rigorously evaluate the model's anomaly detection capability, the test set also included 30,000 additional soil-only spectra, comprising 10,000 samples each for dry soil, 10% moisture, and 20% moisture conditions, that were entirely distinct from the training set. Since the autoencoder had not encountered either landmine-contaminated spectra or these specific soil-only spectra during training, its reconstruction was guided exclusively by its learned representation of typical, unperturbed soil spectra. This setup allowed the model to highlight discrepancies in the landmine spectra as potential anomalies.

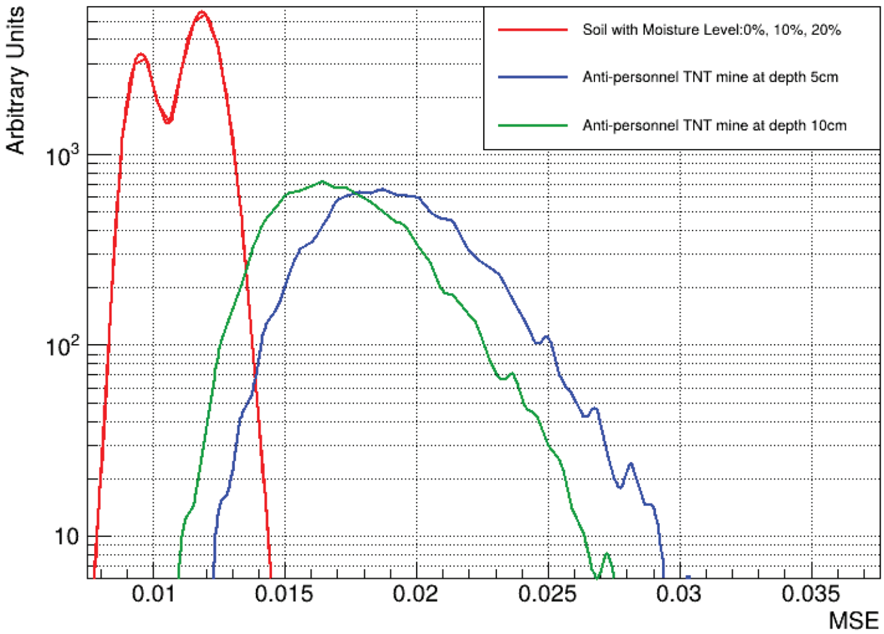

Figure 4 MSE distributions for clean soil spectra (all humidity levels combined) and landmine-buried spectra at 5 cm and 10 cm depths. Clean soil samples show low reconstruction errors, while landmine-affected spectra produce significantly higher MSE values. The clear separation between distributions demonstrates the autoencoder's ability to detect anomalies and supports its use for identifying buried landmines using PGNAA.

The Mean Squared Error (MSE) between each input spectrum and its reconstructed output was used as the reconstruction error, serving as a direct metric for spectral anomaly detection. Spectra corresponding to clean soil samples consistently yielded low MSE values, reflecting high-fidelity reconstructions by the autoencoder. In contrast, spectra from soil containing a buried TNT landmine produced significantly higher MSE values due to the presence of spectral features unfamiliar to the model. Figure 4 illustrates the distribution of reconstruction errors across all test conditions, including the aggregated MSE distribution for clean soil spectra under all three moisture levels (0%, 10%, and 20%), as well as for landmine-influenced spectra at burial depths of 5 cm and 10 cm. A clear statistical separation is evident between the background and anomalous spectra, confirming the model's sensitivity to landmine-induced gamma signatures.

A detection threshold was defined at a reconstruction error of 0.01445, above which an input spectrum is classified as anomalous. This threshold yielded a signal detection efficiency of 97.46% for landmines buried at 5 cm and 87.31% for those at 10 cm. These values reflect the fraction of landmine spectra correctly identified as anomalies while maintaining robust separation from the background soil distributions. The performance drop at 10 cm burial depth can be attributed to the greater attenuation of both neutrons and gamma rays, which reduces the prominence of spectral deviations introduced by the explosive material.

Nevertheless, even at 10 cm depth, the anomaly signal remains distinctly detectable relative to the background, demonstrating the system's potential applicability to a range of buried threat scenarios. These results validate the effectiveness of the CNN autoencoder in detecting subsurface explosives based on prompt gamma spectral anomalies and further support the method's scalability for detecting larger, more easily detectable anti-tank mines in practical field conditions.

Discussion

The results of this study affirm the viability of using a convolutional autoencoder trained solely on simulated prompt gamma spectra from soil to detect anomalies indicative of buried antipersonnel landmines. A critical component of this framework is the $LaBr_3$ detector's ability to resolve high-energy gamma lines, notably the emission from nitrogen—a primary elemental marker in common explosives such as TNT and RDX. To enable this, the detector was simulated with a maximum energy range of 15 MeV, necessitating precise electronic design in practical implementations. Achieving reliable performance at such high energies requires low-noise analog front-end circuitry, high-speed digitisers with extended dynamic range, and probably temperature-compensated calibration systems to ensure energy linearity and resolution. Sensitivity analyses revealed that constraining the detection range, for example by lowering the upper energy limit to 12 MeV to reduce hardware complexity or shielding requirements, results in a measurable decline in detection performance. This is attributed to the attenuation or loss of critical high-energy gamma lines that provide discriminatory power between background soil and explosive-containing spectra.

Despite this, the model still maintains its anomaly detection capability, although with a narrower margin of separation between landmine and background samples in the reconstruction error space. Importantly, while the present evaluation focused on antipersonnel landmines, which are compact, low-metal content devices and thus represent a challenging detection scenario, the methodology is expected to yield even more robust results when applied to larger anti-tank mines. These devices typically contain greater quantities of explosive material and present larger target volumes for neutron interrogation, resulting in stronger gamma-ray signals and higher anomaly contrast. Consequently, the approach outlined here offers a scalable foundation for landmine detection systems, balancing detection sensitivity, spectral resolution, and practical engineering constraints in future experimental or field deployments.

Conclusions

This study presents a novel, simulation-driven approach for detecting buried anti-personnel landmines using prompt gamma spectra generated by 14 MeV neutron interrogation and analysed through a convolutional autoencoder trained exclusively on soil-only spectra. The model successfully identified landmine-induced spectral anomalies across varying soil moisture conditions, without requiring training on explosive data. A detection threshold of 0.01445 in reconstruction error enabled signal detection efficiencies of 97.46% and 87.31% for landmines buried at 5 cm and 10 cm depths, respectively. These results highlight the effectiveness of integrating high-resolution gamma detection with unsupervised deep learning for anomaly detection. Future efforts will focus on expanding the dataset to encompass more diverse soil types and explosive materials, enhancing robustness to environmental noise, and evaluating the method's performance on anti-tank mines and smaller ordnance, with the goal of developing a scalable and field-deployable landmine detection system.

References

Adari, S., and S. Alla. 2024. *Beginning Anomaly Detection Using Python-Based Deep.* Berkeley: Apress.

Agostinelli, S, Allison J., Amako K., Apostolakis J., Araujo H., Arce P., Asai M., et al. 2003. "Geant4—a simulation toolkit." *Nuclear Instruments and Methods A* 506 (3): 250-303. doi:10.1016/S0168-9002(03)01368-8.

Clifford, E.T.H., J.E. McFee, H. Ing, H.R. Andrews, D. Tennant, E. Harper, and A.A. Faust. 2007. "A militarily fielded thermal neutron activation sensor for landmine detection." *Nuclear Instruments and Methods in Physics Research Section A: Accelerators, Spectrometers, Detectors and Associated Equipment* 579 (1): 418-425. doi:10.1016/j.nima.2007.04.091.

Datema, C.P., V.R. Bom, and C.W.E. van Eijk. 2003. "Monte Carlo simulations of landmine detection using neutron backscattering imaging." *Nuclear Instruments and Methods in Physics Research Section A: Accelerators, Spectrometers, Detectors and Associated Equipment* 513 (1-2): 398-402.

Elsheikh, N.A.A. 2018. "Monte Carlo modelling of a neutron-induced gamma-ray sensor for landmine or explosive detection." *Journal of Radiation Research and Applied Sciences* 11 (4): 403–407. https://doi.org/10.1016/j.jrras.2018.08.004.

Gulli, A., and S. Pal. 2017. *Deep learning with Keras.* Packt Publishing Ltd.

Kingma, Diederik P, and Jimmy Ba. 2015. "Adam: A Method for Stochastic Optimization." *arXiv preprint.* doi:10.48550/arXiv.1412.6980.

Landmine and Cluster Munition Monitor. 2024. "Landmine Monitor 2024." https://www.the-monitor.org/reports/landmine-monitor-2024.

Nebbia, Ginacarlo and Juergen Gerl. 2005. "Detection of buried landmines and hidden explosives using neutron, X-ray and gamma-ray probes." *Europhysics News* 36: 119-123. doi:10.1051/epn:2005403.

Viesti, G., M. Lunardon, G. Nebbia, M. Barbui, M. Cinausero, G. D'Erasmo, M. Palomba, A. Pantaleo, J. Obhođaš, and V. Valković. 2006. "The detection of landmines by neutron backscattering: Exploring the limits of the technique." *Applied Radiation and Isotopes* 64 (6): 706-716. doi:10.1016/j.apradiso.2005.12.017.

Xue, Hui, Guang-Yu Shi, De-Dong He, and Si-Yuan Chen. 2022. "Simulation Study on Landmines Detection by Pulsed Fast Thermal Neutron Analysis." *Arabian Journal for Science and Engineering* 47 (1): 879-885. doi:10.1007/s13369-021-05742-0.

Funding Information
This research received no external funding.

Conflict of Interest
The author declares no potential conflicts of interest with respect to the research, authorship, and/or publication of this article.

Data Availability
The data that support the findings of this study are openly available in the Open Science Framework at https://osf.io/udwqp/